J Appl Electrochem (2009) 39:2181–2190
DOI 10.1007/s10800-009-9804-7

ORIGINAL PAPER

Redox thermodynamics of cytochromes *c* subjected to urea induced unfolding

Stefano Monari · Antonio Ranieri · Giulia Di Rocco · Gert van der Zwan · Silvia Peressini · Claudio Tavagnacco · Diego Millo · Marco Borsari

Received: 30 September 2008 / Accepted: 20 January 2009 / Published online: 3 February 2009

Abstract The thermodynamics of the electron transfer (ET) process for beef heart and yeast cytochromes *c* and the Lys72Ala/Lys73Ala/Lys79Ala mutant of the latter species subjected to progressive urea-induced unfolding was determined electrochemically. The results indicate the presence of at least three protein forms which were assigned to a low-temperature and a high-temperature His-Met intermediate species and a bis-histidinate form (although the presence of a His-Lys form cannot be excluded). The much lower $E^{\circ\prime}$ value of the bis-histidinate conformer as compared to His-Met ligated species is largely determined by the enthalpic contribution induced by axial ligand substitution. The biphasic $E^{\circ\prime}$ versus T profile for the His-Met species is due to a difference in reduction entropy between the conformers at low and high temperatures. Enthalpy–entropy compensation phenomena for the reduction reaction at varying urea concentration for all the forms of the investigated cytochromes *c* were addressed and discussed.

Keywords Cytochrome *c* · Electrochemistry · Electron transfer · Unfolding · Thermodynamics · Urea

S. Monari · A. Ranieri · G. Di Rocco · M. Borsari (✉)
Department of Chemistry, University of Modena and Reggio Emilia, via Campi 183, 41100 Modena, Italy
e-mail: marco.borsari@unimore.it

G. van der Zwan · D. Millo
Laser Centre-Analytical Chemistry and Applied Spectroscopy, Vrije Universiteit Amsterdam, De Boelelaan 1083, 1081 HV Amsterdam, The Netherlands

S. Peressini · C. Tavagnacco
Department of Chemistry, University of Trieste, via Giorgieri 1, 34127 Trieste, Italy

1 Introduction

Cytochrome *c* is a single-heme protein which plays a central role in biological electron-transport chains, during which the heme iron switches between the Fe(III)/Fe(II) states [1–3]. The molecular determinants of the formal reduction potential $E^{\circ\prime}$, along with effects of temperature, ionic strength, solvent composition, pH-induced conformational changes and ligand binding have been investigated extensively [4–8]. Significant insight into the functional properties of cytochrome *c* can also be gained from the investigation of the folding and unfolding process, in particular the mechanisms controlling the formation of the functionally active three-dimensional structure of the protein [9–14]. Myer et al. [15] proposed a denaturation mechanism summarized by the scheme:

$$N \rightleftharpoons X_1 \rightleftharpoons X_2 \rightleftharpoons D$$

where N is the native protein (0 M urea) and D a species in which the heme center is coordinated by two His residues (>7 M urea). X_1 and X_2 are two intermediate and partially unfolded forms. The transition $N \rightleftharpoons X_1$ involves loosening of the frontal section of the heme crevice with consequently an increase of heme exposure to the solvent. No change in the heme coordination sphere occurs. The transition $X_1 \rightleftharpoons X_2$ entails conformational perturbations, again without alteration of the coordination of the heme iron. The transition $X_2 \rightleftharpoons D$ involves rupture of the Fe–S(Met80) bond, its substitution with a linkage to another His residue (at neutral pH) or an H_2O molecule (at acidic pH), loosening of the tryptophan-heme domain and an almost complete rearrangement of the polypeptide conformation of the protein. More recently, however, more complicated mechanisms have been proposed [14, 16–21]. Concerted unfolding units (foldons) have been claimed to determine

the folding-unfolding behavior of cytochrome *c* [16–21]. In particular the N-yellow Ω loop (residues 40–57) is suggested to be involved in the first step of the unfolding pathway [21]. Moreover, on the basis of ^{1}H NMR measurements, a non-native form attributed to the replacement of Met80 with one lysine side chain has been observed under mild (partially) denaturing conditions [14]. This form has been proposed to originate the bis-histidinate form under stronger denaturing conditions.

The relationship between protein structure and electron transfer thermodynamics can be better understood through a detailed investigation of the electrochemical aspects of the unfolding processes. For this reason, several studies have been devoted to the characterization of ET processes of cytochrome *c* in solution in the presence of denaturant agents [22–24], and recently the structural perturbation in the heme cavity due to the unfolding processes was investigated through analysis of the reorganization energy λ [25].

In this paper, we have investigated the thermodynamic aspects of the electron transfer process of bovine heart cytochrome *c*, recombinant untrimethylated yeast iso-1-cytochrome *c*, and its triple mutant Lys72Ala/Lys73Ala/Lys79Ala in the presence of urea, a well-known unfolding agent. The residues Lys72, Lys73 and Lys79 are distributed around the heme crevice and are involved in molecular recognition with the redox partners and pH-induced conformational transitions [1–3, 26, 27]. The replacement of these three positively charged residues with neutral ones perturbates the charge distribution on the crevice, affecting the network of hydrogen bonds that is responsible for the stabilization of the protein 3D structure [15, 24].

As a consequence, the unfolding process and the functional properties of the intermediate forms could be remarkably affected by the modification of the charge distribution around the heme crevice. Recent resonance Raman studies have shown that the heme of ferricytochrome *c* at high urea concentration and at neutral pH features a bis-histidine ligation [22]. In the present work, the redox thermodynamics of this protein variant has been characterized and compared with that of the native form. Although the unfolding effect of urea on cytochromes *c* is discussed at a fundamental level, the implications of this systems in biocatalysis are worth considering. In fact, the peroxidase activity of cytochrome *c* increases substantially upon unfolding [28, 29].

2 Experimental procedures

2.1 Materials

Beef heart cytochrome *c* (bhcc, hereafter) was purchased from Sigma and further purified by cation exchange chromatography. Wild type recombinant untrimethylated C102T *Saccharomyces cerevisiae* iso-1-cytochrome *c* (ycc, hereafter) and the variant Lys72Ala/Lys73Ala/Lys79Ala (KtoA, hereafter) were expressed in *E. coli* and purified following the procedures described elsewhere [26, 27, 30], tyrosine replaces the cysteine at position 102 in both species. This substitution prevents dimerization and minimizes autoreduction while resulting in retention of the spectral and the functional properties of the protein [31, 32]. All chemicals were of reagent grade. Urea was purchased from Sigma-Aldrich. Nanopure water was used throughout.

2.2 Electrochemical measurements

A Potentiostat/Galvanostat mod. 273A (EG&G PAR, Oak Ridge, USA) was used to perform cyclic voltammetry (CV, hereafter). Experiments were carried out at different scan rates (0.02–2 V s^{-1}) using a cell for small volume samples (0.5 mL) under argon. A 1 mm-diameter polycrystalline gold wire was used as working electrode, a Pt sheet and a saturated calomel electrode (SCE) as counter and reference electrode, respectively. The electric contact between the SCE and the working solution was achieved with a Vycor® (from PAR) set. Potentials were calibrated against the MV^{2+}/MV^{+} couple (MV = methylviologen) [33]. All the redox potentials reported here are referred to SHE. The working gold electrode was cleaned by flaming it in oxidizing conditions; afterwards, it was heated in concentrated KOH for 30 min then, after rinsing in water, in concentrated sulfuric acid for 30 min. To minimize residual adsorbed impurities, the electrode was subjected to 20 voltammetric cycles between +1.5 and −0.25 V at 0.1 V s^{-1} in 1 M H_2SO_4. Finally, the electrode was rinsed in water and anhydrous ethanol. The Vycor® set was treated in an ultrasonic pool for about 5 min. Modification of the electrode surface was performed by dipping the polished electrode into a 1 mM solution of 4-mercaptopyridine for 30 s, then rinsing it with MILLIQ water. Protein solutions were freshly prepared before use and their concentration (typically 0.2 mM) was carefully checked spectrophotometrically (Jasco mod. V-570 spectrophotometer). 0.01 M NaCl + 0.01 M phosphate buffer at pH 7 were used as base electrolytes and urea concentrations were varied between 0 and 10 M. The formal reduction potentials $E^{o\prime}$ were calculated from the average of the anodic and cathodic peak potentials [33] and found almost independent of scan rate in the range 0.02–2 V s^{-1}. In all cases the linear dependence of i_{pc} on $v^{1/2}$ (v = scan rate) indicates a diffusion controlled electrochemical process. For each species, the experiments were performed at least five times and the reduction potentials were found to be reproducible within ±0.002 V. The CV experiments at different temperatures were carried out with a cell in a

"nonisothermal" setting [33], namely in which the reference electrode was kept at constant temperature (21 ± 0.1 °C) whereas the half-cell containing the working electrode and the Vycor® junction to the reference electrode was under thermostatic control with a water bath. The temperature was varied from 5 to 55 °C. With this experimental configuration, the reaction entropy for reduction of the oxidized protein ($\Delta S_{rc}^{\circ\prime}$) is given by [33–35]:

$$\Delta S_{rc}^{\circ\prime} = S_{red}^{\circ\prime} - S_{ox}^{\circ\prime} = nF\frac{dE^{\circ\prime}}{dT} \quad (1)$$

Thus, $\Delta S_{rc}^{\circ\prime}$ was determined from the slope of the plot of $E^{\circ\prime}$ versus temperature which turns out to be linear consistent with the assumption that $\Delta S_{rc}^{\circ\prime}$ is constant over the limited temperature range investigated. Under the same assumption, the enthalpy change ($\Delta H_{rc}^{\circ\prime}$) was obtained from the Gibbs-Helmholtz equation, namely as the negative slope of the $E^{\circ\prime}/T$ versus $1/T$ plot. The nonisothermal behavior of the cell was checked carefully by determining the $\Delta H_{rc}^{\circ\prime}$ and $\Delta S_{rc}^{\circ\prime}$ values of the ferricyanide/ferrocyanide couple [33–35].

3 Results

The voltammetric response and the temperature dependence of $E^{\circ\prime}$ for bhcc, ycc and KtoA were studied in solution as a function of urea concentration on a polycrystalline gold electrode functionalized with 4-mercaptopyridine. All the proteins show a very similar electrochemical behavior. Typical CV signals obtained for ycc in the presence of 0, 3 and 7 M urea are shown in Fig. 1. The CV curves obtained up to 4 and 2 M urea for bhcc and the other species, respectively, are similar to those recorded in the absence of denaturant: a single quasi-reversible wave (wave I) is observed. The anodic and cathodic currents increase linearly with the square root of the scan rate (not shown), indicating that the electrochemical signal corresponds to a diffusion controlled process. The current ratio i_{pa}/i_{pc} is approximately 1 for all the investigated temperatures and scan rates, and the peak-to-peak separation increases with scan rate. At higher urea concentrations (≥4 M for bhcc, ≥2 M for the other species) a new cathodic peak (wave II) at negative potentials is observed (Fig. 1), which is irreversible at low scan rate (<0.05 V s^{-1}). This wave increases in intensity to the detriment of the cathodic peak of wave I with increasing urea concentration (Fig. 1, Table 1). At urea concentrations above 8 M the cathodic peak of wave I disappears whereas the corresponding anodic counterpart still partially exists. The anodic counterpart of wave II is observed only at high urea concentrations (≥6 M for bhcc, ≥3 M for the other species) and its intensity increases with increasing sweep rate. As for wave I, the cathodic current of wave II linearly increases with the square root of the sweep rate. The $E^{\circ\prime}$ values of waves I and II slightly decrease at increasing the urea concentration (Tables 2, 3 and 4).

At low urea concentrations (<3 M for bhcc, <1 M for the other species), the $E^{\circ\prime}$ value of wave I shows a monotonic linear decrease with increasing temperature

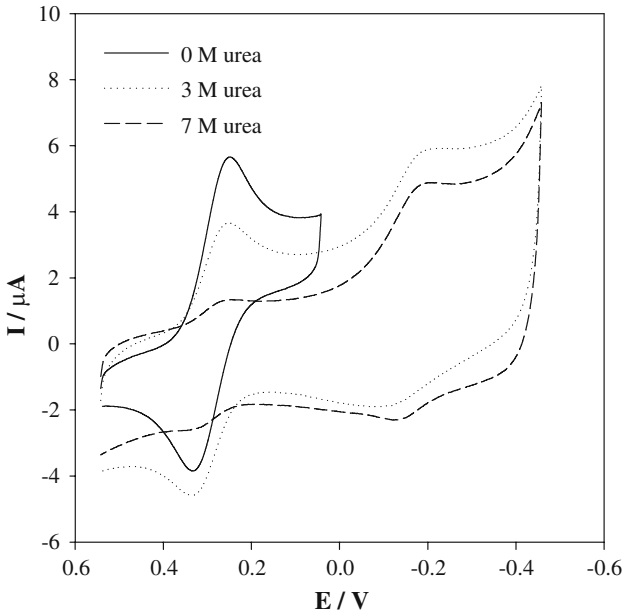

Fig. 1 CV curves of ycc at different urea concentrations. $v = 0.05$ V s^{-1}; base electrolytes: 0.01 M NaCl and 0.01 M phosphate buffer, pH 7, $T = 278$ K

Table 1 Cathodic peak currents of different cytochromes *c* from CV measurements at different urea concentrations

C_{urea} (mol L^{-1})	bhcc		ycc		KtoA	
	i_{pc} (μA)[a] Wave I	i_{pc} (μA)[a] Wave II	i_{pc} (μA)[a] Wave I	i_{pc} (μA)[a] Wave II	i_{pc} (μA)[a] Wave I	i_{pc} (μA)[a] Wave II
0	5.11	0	5.05	0	5.08	0
0.5	5.02	0.04	4.96	0.05	5.01	0.03
1	4.88	0.14	4.82	0.14	4.82	0.17
2	4.67	0.24	4.22	0.63	3.92	0.96
3	4.50	0.27	2.82	1.90	2.65	2.10
4	4.33	0.29	1.67	2.90	1.24	3.35
5	3.85	0.61	1.02	3.39	0.63	3.80
6	2.96	1.32	0.70	3.54	0.39	3.87
7	1.33	2.78	0.49	3.58	0.14	3.95
8	0.60	3.33	0.21	3.67	0.04	3.86
9	0.28	3.47	0.09	3.62	0	3.73

$T = 278$ K, $v = 0.05$ V s^{-1}, base electrolytes: 0.01 M NaCl and 0.01 M phosphate buffer at pH 7

[a] Average error = ±0.02 μA

Table 2 Redox thermodynamic parameters of bhcc at different urea concentrations

C_{urea} (mol L^{-1})	His-Met ligated forms							His-Lys/bis-histidinate forms (at $C_{urea} \geq 8$ mol L^{-1} bis-histidinate form only)		
	Low-T form			High-T form						
	$E^{\circ\prime}$ (V)[a]	$\Delta S^{\circ\prime}_{rc}$ (J mol^{-1} K^{-1})	$\Delta H^{\circ\prime}_{rc}$ (kJ mol^{-1})	T_{break} (K)	$E^{\circ\prime}$ (V)[b]	$\Delta S^{\circ\prime}_{rc}$ (J mol^{-1} K^{-1})	$\Delta H^{\circ\prime}_{rc}$ (kJ mol^{-1})	$E^{\circ\prime}$ (V)[a]	$\Delta S^{\circ\prime}_{rc}$ (J mol^{-1} K^{-1})	$\Delta H^{\circ\prime}_{rc}$ (kJ mol^{-1})
0	0.269	−36	−36.5	–	–	–	–	–	–	–
0.5	0.268	−34	−35.8	–	–	–	–	–	–	–
1	0.267	−35	−36.0	–	–	–	–	–	–	–
2	0.265	−42	−37.8	–	–	–	–	−0.211	37	31.2
3	0.262	−50	−39.9	313	0.232	–[c]	–[c]	−0.213	37	31.4
4	0.258	−58	−41.9	308	0.228	−101	−53.6	−0.215	38	31.9
5	0.256	−60	−42.3	308	0.225	−107	−55.2	−0.217	39	32.4
6	0.254	−61	−42.4	308	0.221	−111	−56.1	−0.219	39	32.6
7	0.253	−62	−42.6	303	0.219	−114	−56.8	−0.220	40	33.0
8	0.252	−63	−42.8	303	0.219	−115	−57.2	−0.221	40	33.0
9	0.251	−64	−43.0	298	0.217	−117	−57.6	−0.222	41	33.4

Base electrolytes: 0.01 M NaCl and 0.01 M phosphate buffer at pH 7. Average errors on $E^{\circ\prime}$, $\Delta S^{\circ\prime}_{rc}$ and $\Delta H^{\circ\prime}_{rc}$ values are ±0.002 V, ±2 J mol^{-1} K^{-1} and ±0.3 kJ mol^{-1}, respectively

[a] $T = 293$ K

[b] $T = 313$ K

[c] Not evaluable

Table 3 Redox thermodynamic parameters of ycc at different urea concentrations

C_{urea} (mol L^{-1})	His-Met ligated forms							His-Lys/bis-histidinate forms (at $C_{urea} \geq 8$ mol L^{-1} bis-histidinate form only)		
	Low-T form			High-T form						
	$E^{\circ\prime}$ (V)[a]	$\Delta S^{\circ\prime}_{rc}$ (J mol^{-1} K^{-1})	$\Delta H^{\circ\prime}_{rc}$ (kJ mol^{-1})	T_{break} (K)	$E^{\circ\prime}$ (V)[b]	$\Delta S^{\circ\prime}_{rc}$ (J mol^{-1} K^{-1})	$\Delta H^{\circ\prime}_{rc}$ (kJ mol^{-1})	$E^{\circ\prime}$ (V)[a]	$\Delta S^{\circ\prime}_{rc}$ (J mol^{-1} K^{-1})	$\Delta H^{\circ\prime}_{rc}$ (kJ mol^{-1})
0	0.260	−43	−37.7	–	–	–	–	–	–	–
0.5	0.259	−43	−37.6	–	–	–	–	–	–	–
1	0.257	−44	−37.7	313	0.243	–[c]	–[c]	–	–	–
2	0.252	−46	−37.8	308	0.238	−77	−47.1	−0.155	54	30.8
3	0.248	−55	−40.0	308	0.232	−84	−48.7	−0.157	54	31.0
4	0.246	−62	−41.9	308	0.228	−97	−52.4	−0.158	55	31.4
5	0.245	−63	−42.1	303	0.226	−101	−53.4	−0.161	55	31.7
6	0.244	−64	−42.3	303	0.223	−105	−54.4	−0.163	56	32.1
7	0.243	−65	−42.5	303	0.222	−107	−54.9	−0.165	57	32.6
8	0.242	−66	−42.7	298	0.222	−108	−55.2	−0.166	57	32.7
9	0.241	−67	−42.9	298	0.218	−110	−55.5	−0.167	58	33.1

Base electrolytes: 0.01 M NaCl and 0.01 M phosphate buffer at pH 7. Average errors on $E^{\circ\prime}$, $\Delta S^{\circ\prime}_{rc}$ and $\Delta H^{\circ\prime}_{rc}$ values are ±0.002 V, ±2 J mol^{-1} K^{-1} and ±0.3 kJ mol^{-1}, respectively

[a] $T = 293$ K

[b] $T = 313$ K

[c] Not evaluable

Table 4 Redox thermodynamic parameters of KtoA at different urea concentrations

C_{urea} (mol L^{-1})	His-Met ligated forms							His-Lys/bis-histidinate forms (at $C_{urea} \geq 8$ mol L^{-1} bis-histidinate form only)		
	Low-T form			High-T form						
	$E^{\circ\prime}$ (V)[a]	$\Delta S^{\circ\prime}_{rc}$ (J mol^{-1} K^{-1})	$\Delta H^{\circ\prime}_{rc}$ (kJ mol^{-1})	T_{break} (K)	$E^{\circ\prime}$ (V)[b]	$\Delta S^{\circ\prime}_{rc}$ (J mol^{-1} K^{-1})	$\Delta H^{\circ\prime}_{rc}$ (kJ mol^{-1})	$E^{\circ\prime}$ (V)[a]	$\Delta S^{\circ\prime}_{rc}$ (J mol^{-1} K^{-1})	$\Delta H^{\circ\prime}_{rc}$ (kJ mol^{-1})
0	0.264	−58	−42.5	–	–	–	–	–	–	–
0.5	0.263	−57	−42.1	–	–	–	–	–	–	–
1	0.262	−58	−42.3	313	0.249	–[c]	–[c]	–	–	–
2	0.256	−63	−43.2	308	0.242	−79	−48.1	−0.163	65	34.8
3	0.251	−70	−44.7	308	0.236	−86	−49.7	−0.165	65	35.0
4	0.248	−76	−46.2	303	0.233	−98	−53.2	−0.167	66	35.5
5	0.247	−77	−46.4	303	0.232	−104	−54.9	−0.169	66	35.6
6	0.246	−78	−46.6	303	0.230	−108	−56.0	−0.171	67	36.1
7	0.246	−79	−46.9	298	0.229	−110	−56.5	−0.174	67	36.4
8	0.245	−80	−47.1	298	0.227	−114	−57.6	−0.176	68	36.9
9	–	–	–	–	–	–	–	−0.177	68	37.0

Base electrolytes: 0.01 M NaCl and 0.01 M phosphate buffer at pH 7. Average errors on $E^{\circ\prime}$, $\Delta S^{\circ\prime}_{rc}$ and $\Delta H^{\circ\prime}_{rc}$ values are ±0.002 V, ±2 J mol^{-1} K^{-1} and ±0.3 kJ mol^{-1}, respectively

[a] $T = 293$ K

[b] $T = 313$ K

[c] Not evaluable

from 5 to 45 °C (Fig. 2a, Tables 2, 3 and 4). The electrochemical process is reversible throughout the temperature range investigated. At higher urea concentrations, the $E^{\circ\prime}$ versus T plots become biphasic with a transition point (T_{break}) depending on the urea concentration (Fig. 2a, Tables 2, 3 and 4). Similar $E^{\circ\prime}$ versus T profiles were previously observed for several cytochromes at alkaline pH values [33, 36–39]. The $E^{\circ\prime}$ versus T plots for wave II for all the investigated proteins show invariably a monotonic linear increase of $E^{\circ\prime}$ with increasing temperature (Fig. 3a, Tables 2, 3 and 4).

The thermodynamic parameters $\Delta S^{\circ\prime}_{rc}$ and $\Delta H^{\circ\prime}_{rc}$ of the redox processes corresponding to waves I and II obtained at different urea concentrations have been calculated from the $E^{\circ\prime}$ versus T (Figs. 2a, 3a) and $E^{\circ\prime}/T$ versus $1/T$ (Figs. 2b, 3b) plots, respectively, and are reported in Tables 2, 3 and 4.

4 Discussion

The slight decrease in the $E^{\circ\prime}$ value of wave I for urea concentrations from 0 to about 9 M indicates that this signal can be attributed to the His-Met ligated cytochrome *c* subjected to moderate conformational perturbations [24]. The appearance of a new wave (wave II) at potentials approximately 0.5 V lower than that of wave I (Fig. 1, Tables 2, 3 and 4) most likely corresponds to the formation of a new conformer with an altered heme iron axial coordination [14, 22–24].

The slight shift in $E^{\circ\prime}$ of wave I observed at increasing urea concentration derives from remarkable and opposite changes in $\Delta S^{\circ\prime}_{rc}$ and $\Delta H^{\circ\prime}_{rc}$ values: this has been shown to be the result of the progressive increase in exposure of the redox center to the solvent with no changes in the coordination sphere of the metal [40–43]. However, here we adopt the model by Myer et al. [15] to interpret the electrochemical behavior of cytochrome *c* in the presence of urea without specific structural considerations which would be rather speculative. Therefore, the $E^{\circ\prime}$ shift at low urea concentration can in principle be correlated with the progressive unfolding of the N-yellow Ω loop [21], but no further info on the role of this foldon can be gained. It is a fact, however, the Myer's model and the "foldons" theory do not conflict.

For the above, wave I can be assigned to the Fe(III)/Fe(II) equilibrium of the heme iron in the native and intermediate species (N, X_1, X_2, vide infra) with the shift in $E^{\circ\prime}$ value corresponding to the progressive transition $N \rightleftharpoons X_{1,2}$. Under our experimental conditions the X_1 and X_2 forms can not be observed individually, probably because the structural and electrochemical properties of X_1 and X_2 are rather similar, as are the electron transfer parameters [24]. The properties of wave II suggest its

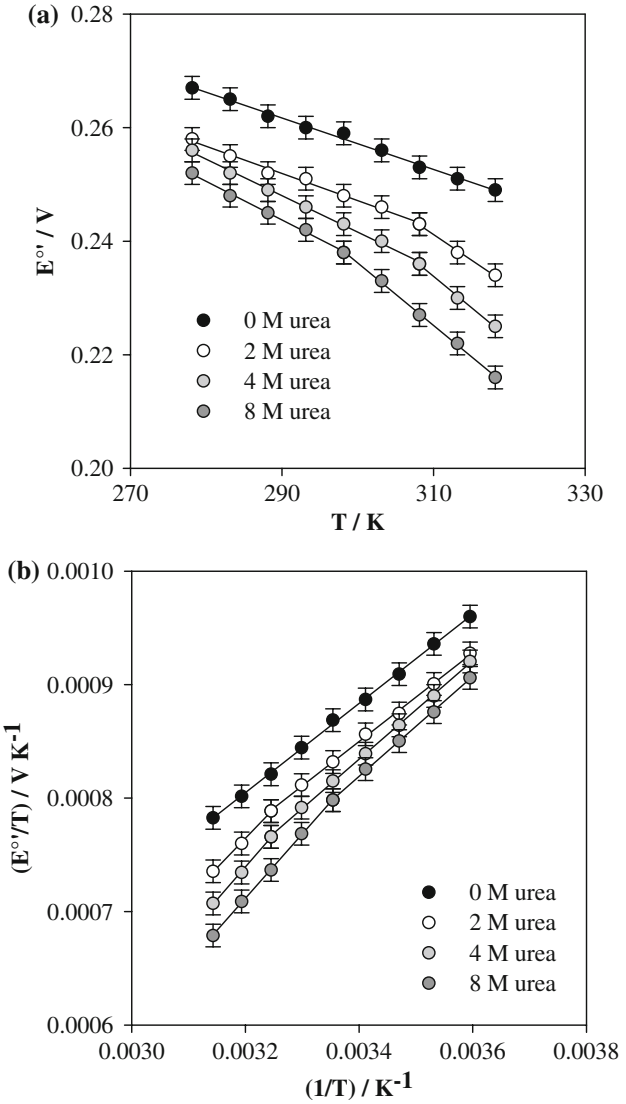

Fig. 2 $E^{\circ\prime}$ versus T (**a**) and $E^{\circ\prime}/T$ versus $1/T$ (**b**) plots for the His/Met ligated forms of ycc at different urea concentrations. Base electrolytes: 0.01 M NaCl and 0.01 M phosphate buffer, pH 7

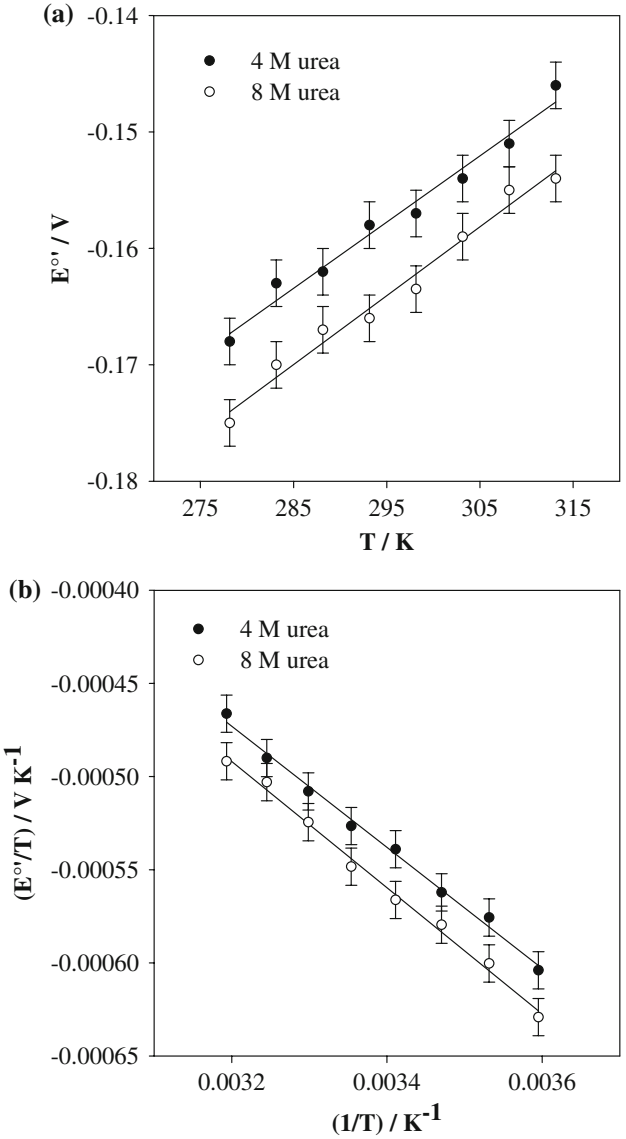

Fig. 3 $E^{\circ\prime}$ versus T (**a**) and $E^{\circ\prime}/T$ versus $1/T$ (**b**) plots for the His-Lys/bis-histidinate forms of ycc at different urea concentrations. At [urea] = 8 M the bis-histidinate species is the only form present in the solution. Base electrolytes: 0.01 M NaCl and 0.01 M phosphate buffer, pH 7

assignment to a species subjected to substitution of the axial ligand Met80 by a harder base such as a nitrogen atom of a histidine or lysine residue. At high urea concentrations ([urea] $\geq$ 8 M) it is well established that a bis-histidinate form of the cytochrome *c* is the prevailing species [14, 22, 23] while at low urea concentrations ($4 <$ [urea] < 8) an equilibrium between a His-Lys form and the bis-histidinate one has been proposed [14].

The more basic character of the nitrogen atom(s) of the histidine (or lysine) ligand compared to the thioether sulfur of the native methionine stabilizes the ferriheme and is likely to be mainly responsible for the dramatic decrease in $E^{\circ\prime}$ value of wave II as compared to wave I. Due to the similar donor properties of the nitrogen from histidine and lysine, the effect of the S $\rightarrow$ N substitution on the $E^{\circ\prime}$ values is expected to be similar for both the aminoacid residues [4, 22–24, 26, 27]. For this reason, an unique CV curve, corresponding to wave II, should be observed when the methionine ligand is substituted by a histidine or lysine. From the electrochemical point of view, the His-Lys and bis-histidinate forms cannot be distinguished. The small decrease in $E^{\circ\prime}$ value observed increasing the urea concentration is consistent, however, with the progressive substitution of the lysine with the histidine. At [urea] $\geq$ 8 M the His-Lys form is no more present and the bis-histidinate species is the only form present in the solution [14, 22–24].

The poor reversibility of wave II (Fig. 1) has already been observed [23, 44] and was attributed to the effects of the cathodic reduction of water occurring in the same potential range corresponding to the reduction of the bis-histidinate form of the cytochromes [23]. At high urea concentrations ([urea] $\geq$ 8) the anodic counterpart of wave II appears and the shape of the CV curves becomes similar to that of a reversible process. The progressive replacement of water molecules at the electrode-solution interface by urea has been suggested to be responsible of the more efficient electron-exchange reaction of the proteins [23]. However, it should be noticed that an increase in the anodic current of wave II can be observed also by increasing the scan rate. The absence and/or the low intensity of the anodic peak could be therefore related also to the instability of both the reduced His-Lys and bis-histidinate forms of the cytochrome *c* which transform rapidly into the reduced His-Met ligated form.

This is not surprising since the reduced form of cytochrome *c* in solution retains its His-Met ligation up to 9 M urea [22, 45] and a similar behavior has been already observed for the "alkaline" form of cytochrome *c* in solution, in which the axial ligand Met80 is substituted by a lysine ligand [33, 46].

All the investigated proteins, therefore, are able to convert to a His-Lys form and then to the bis-histidinate species. The ratio of the cathodic peak currents of waves I and II at each urea concentration can be assumed with good approximation equal to the ratio of the concentrations of His-Met and (His-Lys + bis-histidinate) ligated forms of the cytochrome *c*. As a consequence, under the hypothesis that only these protein species are present at the urea concentrations investigated, the distribution curves of cytochrome forms (Fig. 4) can be easily calculated using the data in Table 1 in which we report the measured cathodic peak currents at different urea concentrations. The decrease in the sum of the cathodic peak currents of waves I and II (Table 1) is probably related to the considerable change in solution viscosity due to the urea addition [23, 44, 47]. From the curves of Fig. 4 it is apparent that the ease of the transition follows the order: KtoA > ycc $\gg$ bhcc. The urea concentrations corresponding to the mid-point of transition result to be about 6.5, 3.5 and 3.2 M for bhcc, ycc and KtoA, respectively. The His-Met form of bhcc shows a remarkably lower propensity toward transition to the His-Lys/His-His forms compared to the other species, according to the behavior already observed for horse heart cytochrome *c* [14, 22, 23].

The $E^{\circ\prime}$ versus T profiles at varying urea concentration (Figs. 2a, 3a; Tables 2, 3 and 4) indicate the presence of several protein forms: the low-T and high-T His-Met intermediate species (X_{LT} and X_{HT}, respectively) and the His-Lys/bis-histidinate forms (D). The X_{LT} to X_{HT} transition occurs at lower temperature for ycc and KtoA compared to bhcc; moreover the T_{break} decreases with increasing urea concentration (Tables 2, 3 and 4). The X_{LT} conformer likely corresponds to the intermediate form(s) $X_{1,2}$ already reported in the literature [15, 22–24] for cytochrome *c* at room temperature (see above) whereas X_{HT} is a different form which should not differ much from the low-T species, on the basis of the similar electrochemical behavior observed.

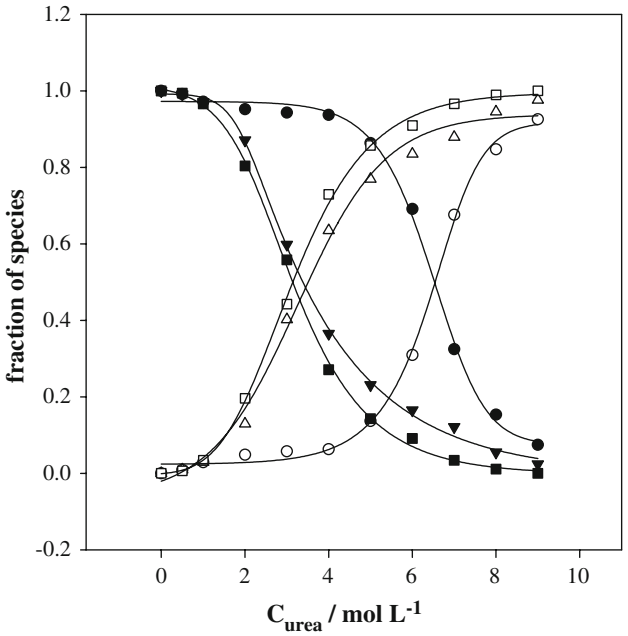

Fig. 4 Distribution curves for the His/Met ligated and the His-Lys/bis-histidinate forms of the investigated cytochromes *c* at different urea concentrations. Base electrolytes: 0.01 M NaCl and 0.01 M phosphate buffer, pH 7; T = 278 K. ● His/Met ligated bhcc, ○ His-Lys/bis-histidinate bhcc, ▼ His/Met ligated ycc, △ His-Lys/bis-histidinate ycc, ■ His/Met ligated KtoA, □ His-Lys/bis-histidinate KtoA

The presence of two T-dependent conformers was already observed for cytochromes *c* from various sources upon increasing pH from slightly acidic or neutral values, but the reason for this transition is not fully understood [33, 36, 37, 39, 48–50]. It has been proposed that this thermal transition involves a conformer with a lower protonation number characterized by a reduced state stabilized on enthalpic bases. However, its $E^{\circ\prime}$ value strongly decreases with increasing temperature due to a much higher entropy loss upon reduction [4, 33, 49]. A greater opening of the heme crevice in the oxidized state as compared to the low-T conformer and reorganizational effects which also include a change in orientation of the axial methionine ligand could be the structural responsible of the observed phenomenon [33, 48].

The unfolding effect corresponding to the $N \rightleftharpoons X_{LT}$ transition would account for the presence of a break

temperature in the presence of urea also at neutral pH. This effect, in fact, could favour the loss of proton(s) responsible for the transition.

For the X_{LT} species, the free energy change for ferriheme reduction ($\Delta G^{\circ\prime}_{rc}$) is determined by opposite enthalpic and entropic contributions (Tables 2, 3 and 4), as observed previously for the *N* form [4, 33]. In this case, the magnitude of each contribution increases markedly with increasing urea concentration but these effects offset each other (compensatory behavior), therefore no relevant changes in $\Delta S^{\circ\prime}_{rc}$ are observed. Solvent reorganization effects, reduction-induced changes in the hydrogen bonding network within the hydration sphere of the cytochrome *c* and in protein flexibility are supposed to play the major role in determining the $\Delta S^{\circ\prime}_{rc}$ values [4, 33, 36–38, 51, 52]. The negative $\Delta H^{\circ\prime}_{rc}$ values, however, mostly arise from the stabilization of the ferroheme by ligand binding interactions and the hydrophobicity of the heme environment, but is also modulated by electrostatic interactions of the heme with protein surface and solution charges [4, 33, 36–38, 51–53]. The slight decrease in the $E^{\circ\prime}$ values observed for the $N \rightarrow X_{LT}$ transition (Tables 2, 3 and 4) can be confidently ascribed to the progressive loosening of the frontal section of the heme crevice induced by urea and, in particular, to the consequent increase in heme exposure to the solvent which stabilizes the oxidized form of the protein [4, 15, 22–24, 33, 36–38, 51, 52]. The corresponding $\Delta S^{\circ\prime}_{rc}$ and $\Delta H^{\circ\prime}_{rc}$ values, however, show a much larger variability with increasing urea concentration (Tables 2, 3 and 4). This result can be ascribed to the occurrence of enthalpy-entropy compensative phenomena in the reduction process of the progressively unfolded cytochrome *c*. These phenomena are well-known in several chemical contexts, when the process involves alteration of weak inter- or intramolecular interactions [54–60]. In the reaction thermodynamics, compensative phenomena imply the existence of a linear relationship between the enthalpy and entropy changes within the considered series of homologous processes [54–60]. An exact compensation would imply a straight line of unit slope at fixed temperature. In water solutions, reorganization effects of the H-bond network in the solvation sphere have been proposed to be the main cause of enthalpy-entropy compensation phenomena [40, 54, 56, 59, 60]. The enthalpic contributions to $\Delta G^{\circ\prime}_{rc}$ ($\Delta H^{\circ\prime}_{rc}$) plotted against the entropic terms at 293 K ($T \cdot \Delta S^{\circ\prime}_{rc}$) for the $N \rightarrow X_{LT}$ transition of each investigated protein at different

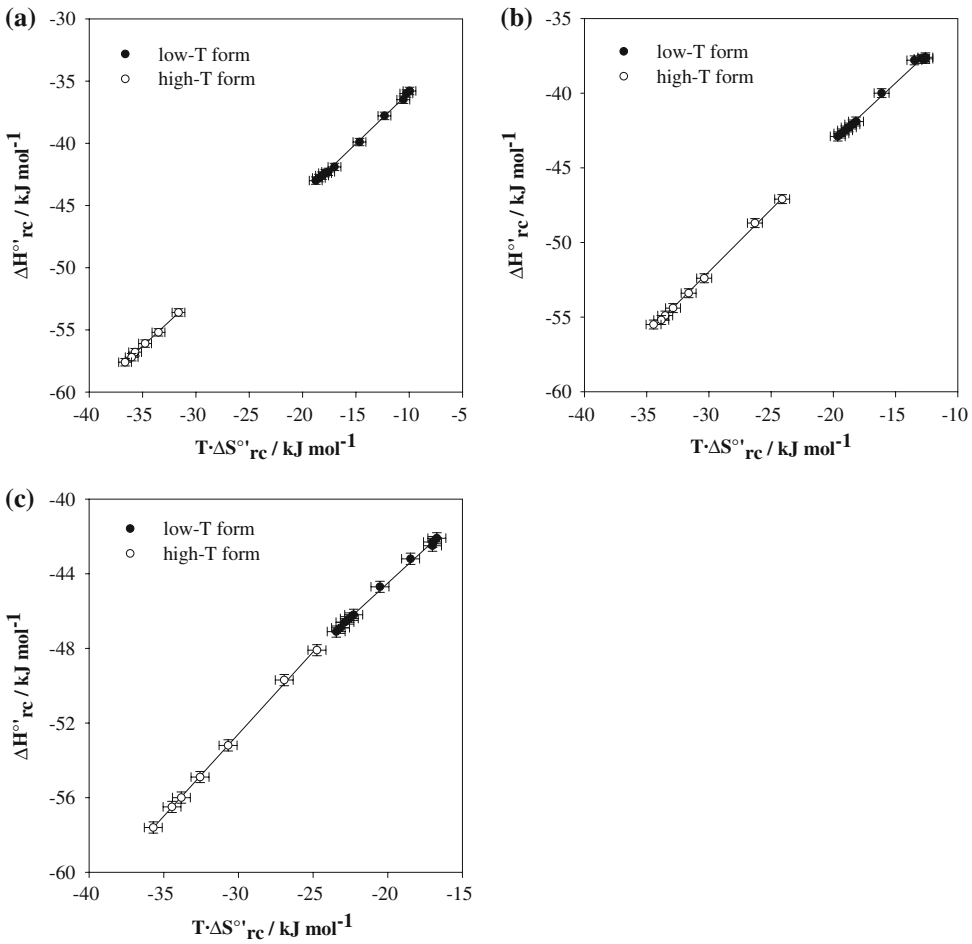

Fig. 5 Enthalpy–entropy compensation plots at different urea concentrations for the reduction thermodynamics of the His/Met ligated forms of bhcc (**a**), ycc (**b**) and KtoA (**c**) at 293 K (●) and 313 K (○). Base electrolytes: 0.01 M NaCl and 0.01 M phosphate buffer, pH 7

urea concentrations is reported in Fig. 5. In all cases, the data points exhibit a linear behavior. It is apparent that the data of Fig. 5 cover ranges which are much greater than the experimental uncertainties, indicating that the resulting compensation patterns are significant [54, 56, 61]. At 293 K, the least-square fittings of $\Delta H^{\circ\prime}_{rc}$ versus $T \cdot \Delta S^{\circ\prime}_{rc}$ for the studied proteins yield slopes of 0.83, 0.78, 0.74 and regression coefficients (r^2) of 0.998, 0.995, 0.997 for bhcc, ycc and KtoA, respectively. Observation of slopes close to unit indicates that for the $N \rightarrow X_{LT}$ transition the contributions to the changes in $\Delta H^{\circ\prime}_{rc}$ and $\Delta S^{\circ\prime}_{rc}$ arising from the reduction-induced reorganization of the H-bond network at the protein-solvent interface (which are fully compensative [54–56, 59]) are much greater than the non-compensating terms associated with the intrinsic chemical process responsible for the stabilization of cytochrome *c* in the oxidized state. Although information about the structural aspects of the H-bond network reorganization involved in the $N \rightarrow X_{LT}$ transition are not available yet, direct interaction of urea molecules with the cytochrome *c* surface and substitution of water molecules at the protein-solvent interface probably play an important role in the compensative change of the thermodynamic parameters. The absence of perfect compensation is most likely related to the fact that the variations in reduction enthalpy depend also on changes in electrostatics at the metal site and the selective stabilization of the oxidized heme by the increasing solvent exposure [4, 33, 36–38, 51–53]. In the case of the $N \rightarrow X_{HT}$ transition, the compensation plots also exhibit good linear trends (Fig. 5, at $T = 313$ K bhcc, ycc and KtoA feature slopes of 0.80, 0.84, 0.88 and regression coefficients r^2 of 0.998, 0.998, 0.997, respectively). Moreover, the data points for the X_{LT} and X_{HT} species are fitted by straight lines with nearly the same slope (Fig. 5). This observation supports extension of the above considerations on the compensative behavior for the X_{LT} species also to X_{HT} and, most notably, indicates that the structural changes responsible for the temperature-induced transition affect the H-bond network at the protein-solution interface but the effect of the unfolding agent concentration on the thermodynamic parameters is nearly the same independently of the nature of the His-Met ligated form. In fact, the $\Delta S^{\circ\prime}_{rc}$ and $\Delta H^{\circ\prime}_{rc}$ values are different for the X_{LT} and X_{HT} species but show the same behavior upon changing urea concentration.

The thermodynamic data for the bis-histidinate form of cytochrome *c* ([urea] $\geq$ 8, [14, 22–24]) allow further insight into the determinants of the remarkably lower reduction potential of this form compared to the His-Met ligated one. The change in axial ligation plays the dominant role in determining the negative $E^{\circ\prime}$ value [22–25], as already observed previously for the alkaline form, in which the nitrogen atom of a lysine residue replaces the sulphur atom of the methionine ligand [2–4, 33]. In fact, the data reported in Tables 2, 3 and 4 indicate that the dramatic decrease in $E^{\circ\prime}$ is determined prevalently by the enthalpic contribution, which is similar for all the proteins investigated and determines the selective stabilization of the oxidized state. Other factors, such as changes in solvation properties, are likely to contribute to this effect as suggested by the large differences in the $\Delta S^{\circ\prime}_{rc}$ values (Tables 2, 3 and 4) [4, 33, 46, 52]. We note that the $E^{\circ\prime}$ and $\Delta S^{\circ\prime}_{rc}$ values for the bis-histidinate species differ somewhat for the various species (Tables 2, 3 and 4), but the differences are larger than those for the His-Met ligated forms (Tables 2, 3 and 4). This suggests that the H-bond networks on the protein surface for the bis-histidinate form are more species-dependent than the His-Met ligated forms. The large unfolding phenomena associated with the transition to the bis-histidinate form and different relaxation properties [15, 22, 23, 62] could be responsible for the above specificity in the redox thermodynamics.

Acknowledgements This work was performed with the financial support of MIUR (COFIN 2007, protocollo 20079Y9578_002, Bioelettrochimica: trasferimento di carica in sistemi di rilevanza biologica) and of the University of Modena and Reggio Emilia.

References

1. Messerschmidt A, Huber R, Poulos T, Wieghardt K (eds) (2001) Handbook of metalloproteins. Wiley, Chichester, UK
2. Scott RA, Mauk GA (eds) (1996) Cytochrome *c*: a multidisciplinary approach. University Science Books, Sausalito, CA
3. Moore GR, Pettigrew GW (eds) (1990) Cytochromes *c*: evolutionary, structural, and physicochemical aspects. Springer-Verlag, Berlin
4. Battistuzzi G, Borsari M, Sola M (2001) Eur J Inorg Chem 2989
5. Bond AM (1994) Inorg Chim Acta 226:293
6. Hill HAO, Hunt NI (1993) Methods Enzymol 227:501
7. Armstrong FA (1990) Struct Bonding 72:137
8. Armstrong FA, Hill HAO, Walton NJQ (1986) Rev Biophys 18:261
9. Bryngelson JD, Onuchic JN, Socci ND, Wolynes PG (1995) Proteins 21:167
10. Dobson CM, Sali A, Karplus M (1998) Angew Chem Int Ed 37:868
11. Dobson CM, Karplus M (1999) Curr Opin Struct Biol 9:92
12. Yeh SR, Rousseau DL (1998) Nat Struct Biol 5:222
13. Xu Y, Mayne L, Englander SW (1998) Nat Struct Biol 5:774
14. Russell BS, Melenkivitz R, Bren KL (2000) Proc Natl Acad Sci USA 97:8312
15. Myer YP, MacDonald LH, Verma BC, Pande A (1980) Biochemistry 19:199
16. Bai Y, Sosnick TR, Mayne L, Englander SW (1995) Science 269:192
17. Bai Y, Englander SW (1996) Proteins Struct Funct Genet 24:145
18. Sinibaldi F, Piro MC, Howes BD, Smulevich G, Ascoli F, Santucci R (2003) Biochemistry 42:7604
19. Milne JS, Xu Y, Mayne L, Englander SW (1999) J Mol Biol 290:811
20. Hoang L, Bedard S, Krishna MMG, Lin Y, Englander SW (2002) Proc Natl Acad Sci USA 99:12173

21. Krishna MMG, Lin Y, Rumbley JN, Englander SW (2003) J Mol Biol 331:29
22. Fedurco M, Augustynski J, Indiani C, Smulevich G, Antalík M, Bánò M, Sedlak E, Galscock MC, Dawson JH (2004) Biochim Biophys Acta 1703:31
23. Fedurco M, Augustynski J, Indiani C, Smulevich G, Antalík M, Bánò M, Sedlak E, Galscock MC, Dawson JH (2005) J Am Chem Soc 127:7638
24. Pilard R, Haladjian J, Bianco P, Serre P-A, Brabec V (1983) Biophys Chem 17:131
25. Shafiey H, Ghourchian H, Mogharrab N (2008) Biophys Chem 134:225
26. Battistuzzi G, Borsari M, De Rienzo F, Di Rocco G, Ranieri A, Sola M (2007) Biochemistry 46:1694
27. Rosell FI, Ferrer JC, Mauk AG (1998) J Am Chem Soc 120:11234
28. Diederix REM, Ubbink M, Canters GW (2002) Biochemistry 41:13067
29. Wang L, Waldeck DH (2008) J Phys Chem C 112:1351
30. Pollock WBR, Rosell FI, Twitchett MB, Dumont ME, Mauk AG (1998) Biochemistry 37:6124
31. Cutler RJ, Pielak GJ, Mauk AG, Smith M (1987) Protein Eng 1:95
32. Liang N, Mauk AG, Pielak GJ, Johnson JA, Smith M, Hoffmann B (1988) Science 240:311
33. Battistuzzi G, Borsari M, Sola M, Francia F (1997) Biochemistry 36:16247
34. Yee EL, Cave RJ, Guyer KL, Tyma PD, Weaver MJ (1979) J Am Chem Soc 101:1131
35. Yee EL, Weaver MJ (1980) Inorg Chem 19:1077
36. Taniguchi I, Iseki M, Takaki E, Toyosawa K, Yamaguchi H, Yasukouchi K (1984) Bioelectrochem Bioenerg 13:373
37. Taniguchi I, Funatsu T, Iseki M, Yamaguchi H, Yasukouchi K (1985) J Electroanal Chem 193:295
38. Koller KB, Hawkridge FM (1988) J Electroanal Chem 239:291
39. Ikeshoji T, Taniguchi I, Hawkridge FM (1989) J Electroanal Chem 270:297
40. Battistuzzi G, Borsari M, Di Rocco G, Ranieri A, Sola M (2004) J Biol Inorg Chem 9:23
41. Battistuzzi G, Bellei M, Borsari M, Canters GW, de Waal E, Jeuken LJC, Ranieri A, Sola M (2003) Biochemistry 42:9214
42. Liu XJ, Huang YX, Zhang WJ, Fan GF, Fan CH, Li GX (2005) Langmuir 21:375
43. Bellei M, Jacopitsch C, Battistuzzi G, Sola M, Obinger C (2006) Biochemistry 45:4768
44. Bixler J, Bakker G, McLendon G (1992) J Am Chem Soc 114:6938
45. Bhuyan AK, Udgaonkar JB (2001) J Mol Biol 312:1135
46. Barker PD, Mauk AG (1992) J Am Chem Soc 114:3619
47. Perl D, Jacob M, Bánò M, Stupák M, Antalík M, Schmid FX (2002) Biophys Chem 96:173
48. Hagarman A, Duitch L, Schweitzer-Stenner R (2008) Biochemistry 47:9667
49. Christen RP, Nomikos SI, Smith ET (1996) J Biol Inorg Chem 1:515
50. Yuan X, Hawkridge FM, Chlebowski JF (1993) J Electroanal Chem 350:29
51. Battistuzzi G, Loschi L, Borsari M, Sola M (1999) J Biol Inorg Chem 4:601
52. Bertrand P, Mbarki O, Asso M, Balnchard L, Guerlesquin F, Tegoni M (1995) Biochemistry 34:11071
53. Battistuzzi G, Borsari M, Cowan JA, Eicken C, Loschi L, Sola M (1999) Biochemistry 38:5553
54. Grunwald E, Steel C (1995) J Am Chem Soc 117:5687
55. Grunwald E (1986) J Am Chem Soc 108:5726
56. Liu L, Guo Q-X (2001) Chem Rev 101:673
57. Searle MS, Westwell MS, Williams DH (1995) J Chem Soc Perkin Trans 2:141
58. Rekharsky M, Inoue Y (2000) J Am Chem Soc 122:4418
59. Liu L, Yang C, Guo Q-X (2000) Biophys Chem 84:239
60. Blokzijl W, Engberts JBNF (1993) Angew Chem Int Ed Engl 32:1545
61. Kita F, Adam W, Jordan P, Nau WN, Wirz J (1999) J Am Chem Soc 121:9265
62. Yeh S-R, Han S, Rousseau DL (1998) Acc Chem Res 31:727